Roughness and wettability control of soda-lime silica glass surfaces by femtosecond laser texturing and curing environments

Anis Ouchene, Guilhem Mollon, Maelig Ollivier, Xxx Sedao, Alina Pascale-Hamri, Guillaume Dumazer, Eric Serris

Graphical Abstract

Roughness and Wettability Control of Soda-Lime Silica Glass Surfaces by Femtosecond Laser Texturing and Curing Environments

Anis Ouchene, Guilhem Mollon, Maelig Ollivier, Xxx Sedao, Alina Pascale-Hamri, Guillaume Dumazer, Eric Serris

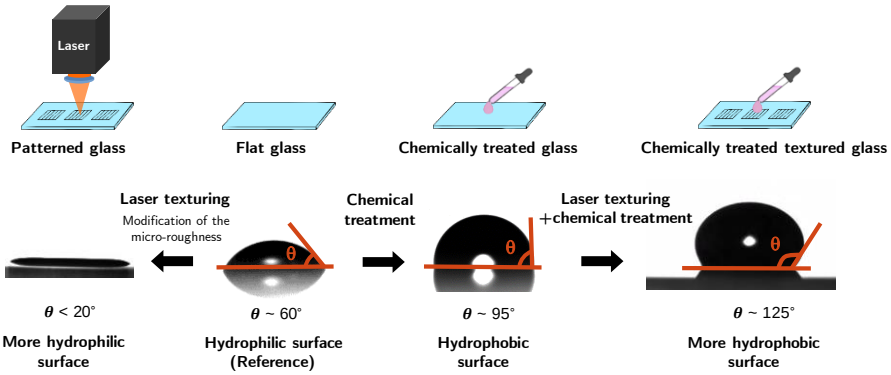

Roughness and Wettability Control of Soda-Lime Silica Glass Surfaces by Femtosecond Laser Texturing and Curing Environments

Anis Ouchene[a], Guilhem Mollon[b], Maelig Ollivier[a], Xxx Sedao[c,d], Alina Pascale-Hamri[d], Guillaume Dumazer[a], Eric Serris[a]

[a]*Mines Saint-Étienne, Univ Lyon, UMR 5307 LGF, Centre SPIN, Saint-Étienne, 42023, France*
[b]*INSA Lyon, Univ Lyon, UMR 5259 LaMCoS, Villeurbanne cedex, 69621, France*
[c]*Laboratoire Hubert Curien, Univ Lyon, Univ Jean Monnet, UMR 5516, Saint-Étienne, 42000, France*
[d]*MANUTECH-USD, 20 rue du Professeur Benoit Lauras, Saint-Étienne, 42000, France*

Abstract

The influence of laser texturing parameters and chemical curing environments on the wettability of flat soda-lime silica glass surfaces was studied by contact angle measurements. The surfaces were textured using femtosecond laser pulses with varying fluence, periodicity, and pulse number. By exposing these textured surfaces to different chemical curing environments, a range of hydrophilicity and hydrophobicity was observed. Experimental characterizations of the roughness produced by the texturing, using the optical profilometer, and contact angle hysteresis measurements showed a transition from a Wenzel regime to a Cassie-Baxter regime, induced by the chemical environment.

Keywords: Femtosecond laser texturing, Hydrophobic glass surfaces, Patterned surfaces, Roughness, Wettability, Wenzel's model, Cassie-Baxter's model

Email address: anis.ouchene@mines-stetienne.fr

May 22, 2023

1. Introduction

In the past decades, several research works have been carried out on the wettability and super-hydrophobic behavior of solid surfaces (1). More recently research works are focusing on oil water separation problems (2), anti-icing or self-cleaning surfaces (3), water resistent, anti-fogging or anti-corrosion properties (4).

The wetting of surfaces is characterized by a contact angle θ_c determined by the Young-Dupré relation (5):

$$\cos\theta_c = \frac{\gamma_{SG} - \gamma_{SL}}{\gamma_{LG}}, \tag{1}$$

where γ_{SG}, γ_{SL} and γ_{LG} are the surface tensions of the solid/gas, solid/liquid, and liquid/gas interfaces, as illustrated in Figure 1.a. When the contact angle θ_c is less than 90^o, the surface is designated hydrophilic, whereas a contact angle value greater than 90^o designates hydrophobic surfaces. An even larger value of contact angle $\theta_c \geq 150^o$ designate superhydrophilic surfaces. In a first approximation, the interaction between a rough surface and a water drop can be considered to follow one of the two following idealized extreme states : the Wenzel state (6; 7) or the Cassie-Baxter state (8).

The Wenzel state (Fig 1.b) shows that the drop wets the entire solid surface and seeps into the roughness of the surface. We can write this state by the following relation :

$$\cos\theta = r\cos\theta_c, \tag{2}$$

where $r = S_r/S_a$ (Fig 2.a) is the roughness parameter defined as the ratio of the area of the rough surface S_r to that of apparent surface S_a. As we are on a rough surface the value of $r = S_r/S_a$ is greater than 1. If the wetting property of an idealized flat surface without roughness is hydrophilic (i. e. $\theta_c < 90^o$), the contact angle on the rough surface is decreased as the cosine function is monotonously decreasing from 0 to 180^o and crosses zero for $\theta_c = 90^o$. The hydrophilic property is accentuated by the roughness. Conversely, if the idealized flat surface is hydrophobic, the hydrophobic property will be accentuated by the roughness. The Cassie-Baxter state (Fig. 1.c) shows that the drop remains at the top of the textures, air being trapped in the openings. This state follows the relation :

$$\cos\theta = f\left(\cos\theta_c + 1\right) - 1, \tag{3}$$

where f is the fraction of the solid surface on which the drop rests (Fig 2.b).

The hysteresis of the contact angle is also an important parameter in order to establish the wettability regime of a surface and to understand the geometry of a drop resting on it (9). The hysteresis of the contact angle $\delta\theta$ is defined by the difference between an advancing angle and a receeding

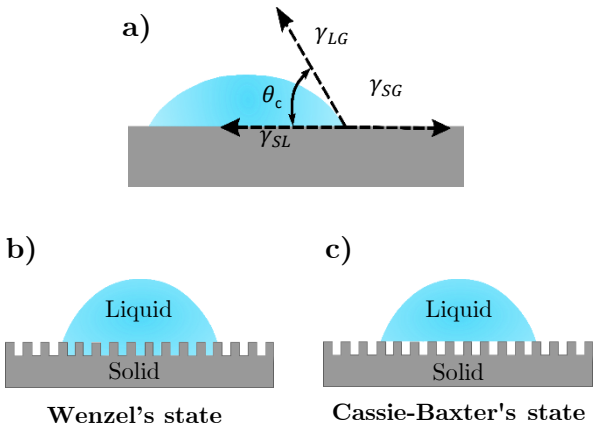

Figure 1: The behavior of the liquid drop on a smooth surface; a) The measurement of the contact angle associated with the Young-Dupré equation (1). The behavior of a liquid drop on a rough surface; b) Wenzel's state on a rough surface, where the drop penetrates into the interstices between the engravings. c) Cassie Baxter's state, where the drop rests on a mixture of solid surface and air is trapped between the grooves.

angle of a gravity driven drop on an inclined surface. In the case of a Cassie-Baxter state where the drop is not anchored in the grooves, the contact angle hysteresis is low and the drop can easily move. On the other hand in the Wenzel state where the drop interacts with the whole texture of the surface, the hysteresis is important and the drop requires more force to move (9; 10).

Modifying the texture of the solid surface is also one way to modify and control its wettability. Various technologies can be used to perform solid surface texturing. Ablation of interfacial matter in a controlled manner can be achieved by femtosecond laser texturing, which can produce modifications of surface properties of metals (12). A mechanical texturing can be produced by applying a stress deformation to the surface by means of micro-knurling. A comparison with the femtosecond laser texturing approach has shown on

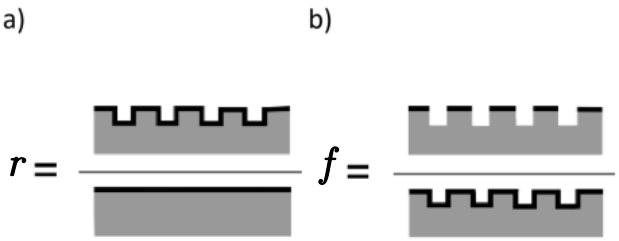

Figure 2: Explanatory schematics for the calculation of the Wenzel roughness r (a) and the Cassie-Baxter fraction of wetted surface f (b) from morphological profiles of the textured surface.

aluminum surface a change in surface wettability (15).

Ion or plasma etching are techniques that can also produce complex texturing(16). Although these techniques have been developed for texturing large number of microchannels on silicon wafer surfaces, they can successfully be applied to glass surfaces (17). However the complex sample preparation, as well as the lack of established etching know-how on curved surfaces makes this technique less flexible to the purpose of this study.

Along the perspective of achiving extreme wettabilities a series of works have been devoted to study natural surface properties in order to understand the complex interplay between texture and chemical properties (11). In particular vegetal surfaces exhibit multiscaled roughness which maximize water repelling. Bio-inspired surfaces of PDMS (Polydimethylsiloxane) can then be produced to achieve similar behaviour (14).

Multiscale roughness produced by femtosecond laser texturing on metal surface was created to test several wettability models (13).

The wettability of textured metals has been extensively studied (18). In

particular the femtosecond laser texturation has been shown to affect the wettability of metal alloys and oxides (12; 19; 20) by modifying the wetting regime parameters, or even crossing over from one wetting regime to another.

Modifications of the surface chemistry induced by the laser texturing of metallic surfaces has been observed on various steel and titanium alloys (18; 21). XPS (X-ray Photoelectron Spectroscopy) put in evidence that the hydrophobic carbon load on the surface increases after laser treatment, and that hydrophilic C-H bond decreases. Complex surface kinetic processes subsequent to the laser treatment, with a transient hydrophilicity of freshly treated surfaces, gradually turn into hydrophobicity over time, as observed in (18; 22).

Most studies on the effect of solid surface texturing on its wettability are focused on metallic or polymeric surfaces (23). Studies of wettability of glasses already proved several decades ago that the functional groups located at the glass surface controls the surface energy, hence the glass wettability (24). In particular the silanol groups on glass have a hydrophilic effect, explaining the water wettability of glasses with a contact angle lower than 90^o. Heat treatment or laser irradiation lead to the transformation of hydrophilic silanol groups into hydrophobic siloxane through a dehydroxylation reaction (24; 25), leading to a decreasing wettability. Chemical treatment can also be used to modify more strongly the wettability of a glass substrate to replace the silanol groups with even more hydrophobic groups such as dichloro-dimethyl-silane among others (26).

In this work we are addressing the question of determining the wetting regime for textured soda-lime silica glass plates. We used a femtosecond

laser irradiation to control the texture of the glass substrate and we tested several curing environnements. Experimental measurements of contact angle of water droplets deposited on the surface are compared with the prediction from both Cassie-Baxter and Wenzel regimes.

2. Materials and Methods

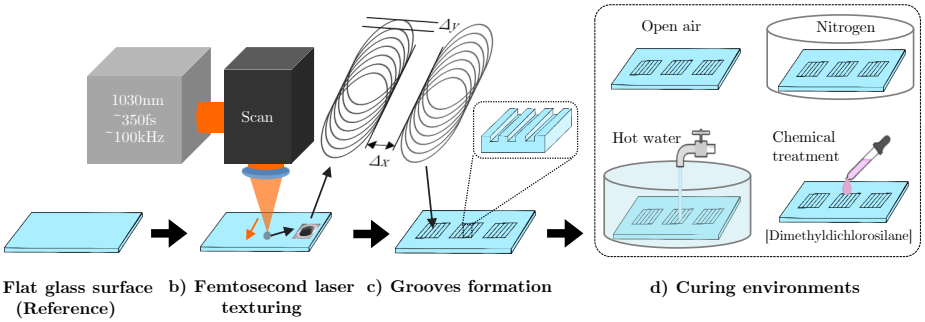

Figure 3: A schematic layout of the femtosecond laser processing system and curing environments. a) A sketch of the reference glass slide. b) A diagram explaining the production of grooves by femtosecond laser texturing following the scan path shown with Δx and Δy. c) The depth and periodicity of the grooves are dependent on the laser parameters used in their creation. d) Each textured glass slide was replicated to be cured in four different chemical environments.

Glass microscope slides (thermo scientific ISO 8037/1 soda-lime glass) with a thickness of approximately 1 mm were used (Fig.3.a). The samples underwent a pre-treatment step of being rinsed with isopropanol before undergoing laser texturing. Afterwards, they were exposed to different curing environments.

2.1. Surface Laser Irradiation

The sample surfaces were subjected to femtosecond laser irradiation using a Tangerine HP fiber laser system by Amplitude Laser Group, with a central wavelength of 1030 nm, a pulse duration of 350 fs, and a repetition rate tunable from single shot to 2 MHz (28; 29). The laser beam was focused to a size of 30 μm using a 100 mm telecentric f-theta lens, and the linearly polarized laser pulses were attenuated and sent through a galvanometer scanner. The overlap ratio of 0.82 between successive laser pulses and between successive laser scan tracks was kept constant for all the experiments. The samples were irradiated at normal incidence under air conditions

Grooves were created on the sample surfaces using fluences of 13.6, 27.69, and 48.43 J/cm^2. For each fluence, three different groove periodicities (40, 60, and 80 μm) and three different passage numbers (5, 10, and 20) were tested, resulting in 9 textured glass slides, each having a unique combination of fluence, periodicity, and number of passages, as shown in Figure 3.*c*.

The parameters of the method were chosen based on the goal of the study, which was to create a range of textures on the sample surfaces and analyze their effect on surface properties. The values of fluence and overlap ratio were chosen to cover a range of groove densities and sizes, allowing for the comparison of the effects of these parameters on the properties of textured surfaces. The values of periodicity and passage number were chosen to explore a wide range of surface textures.

2.2. Curing environments

The influence of different curing environments on the contact angle of the textured samples was studied by replicating each sample into four as shown in Figure 3.*d*. These replicated samples were subjected to the following curing environments:

Hot water: The samples were placed in an ultrasonic deionized water bath at a temperature of 50°C.

Nitrogen: The samples were placed in bags under a nitrogen environment.

Open air: The samples were left in a sample holder in open air.

Chemical treatment: The samples were treated with a silanization solution [Dimethyldichlorosilane] and placed under a chemical hood.

The effect of the different curing envionments on the wettability of untextured glass surfaces is shown by the reference red line in Fig.7. For hot water, nitrogen or air-cured glass surface without texturing the surface properties remain hydrophilic, as explained by the hydroxyl functional groups density at the glass surface (27).

The reader should keep in mind the variability in contact angle measurements of about $\pm 5^o$, as well as the distinct chemical reactivity between the curing environment and the glass surface or the remaining chemical species issued from the pre-treatment. In comparison glass surfaces treated with a silanization solution exhibit hydrophobic properties, as hydroxyl groups are replaced by silane-groups.

2.3. Contact Angle Measurements

One week after the texturing process, contact angles were measured using the sessile drop method. Distilled deionized water was dispensed in 3 μL droplets onto the sample surfaces, and images of the drops were captured and analyzed using the GBX software to determine the contact angle. The measurements were taken at a temperature of 23°C and a humidity of 33 g/m^3. In this study, we have a specific focus on the contact angle measured in the direction perpendicular to the grooves.

2.4. Contact Angle Hysteresis Measurements

There are three distinct experimental methods for determining contact angle hysteresis (30; 31; 32; 33). The first method is the Tilted Plate Method (31), where the advancing and receding contact angles of a water droplet are measured as it begins to slide down an inclined surface.

The Wilhelmy Method (34) is the second method, where a surface is dipped into a water bath and then removed.

Finally, the Sessile Drop Method (30; 31) is the third method we used. This method involves pumping liquid into a droplet, then removing it to measure the advancing angle, followed by the receding angle.

2.5. Surface Topography

The surface topography of the textured surfaces was characterized using chromatic confocal microscopy. This method allowed us to accurately measure the height of the grooves and the width of their openings, providing valuable information about the surface morphology. An example of obtained data is illustrated in Figure 4.

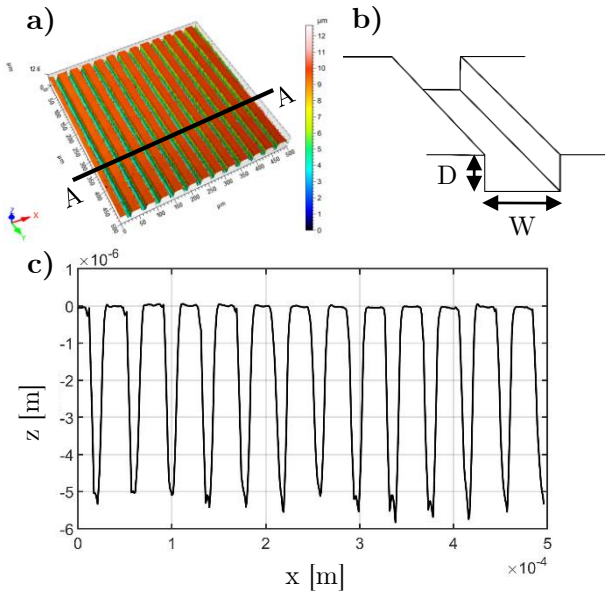

Figure 4: a) 3D profile of the surface obtained by confocal microscopy (Stil) for a textured blade with a fluence of 13.6 J/cm^2, a periodicity of 40 μm, and a passage number of 5. b) A sketch of a groove to show its depth and width. c) The average profile of the textured surface in the direction perpendicular to the grooves (A-A).

By analyzing the surface topography, we were able to gain insights into the morphological features of the textured surfaces and how they were influenced by the laser processing parameters. This information will be useful for optimizing the laser texturing process for specific applications.

3. Results

3.1. Impact of Laser Parameters on Surface Topography

The glass surfaces were textured using a femtosecond laser, resulting in grooves of varying depths and widths. The surface topography was characterized using confocal chromatic microscopy (Stil), as shown in Figure 4,

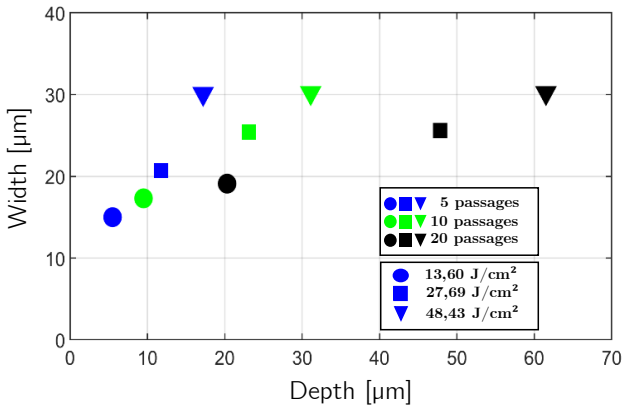

Figure 5: Variation of groove width with depth for textured surfaces with different number of passages and fluences.

which presents a textured slide with a fluence of 13.6 J/cm^2, a periodicity of 40 μm, and 5 laser passages.

We analyzed the effect of laser parameters such as the number of passages and fluence on the topographic parameters of the textured surfaces in Figure 5. The graph displays that the depth and width of the grooves are impacted by laser parameters, as expected. The width of the grooves increases slightly with the number of passages and significantly with the fluence, whereas the depth is more influenced by the number of passages.

To further illustrate this trend, Figure 6 shows the profiles of three grooves formed on samples textured with a fluence of 13.6 J/cm^2 and with #5, #10, and #20 laser passages. The figure demonstrates that the depth of the grooves increases with the number of passages, whereas the width changes only slightly.

After investigating the impact of laser parameters on the topographic parameters of the textured glass surfaces, we turned our attention to the

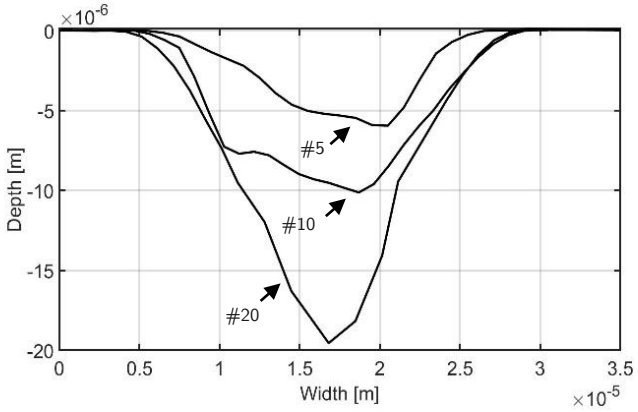

Figure 6: Single groove profiles with a moving average calculated from samples textured at $13.6 J/cm^2$ and with #5, #10, and #20 number of passages.

relationship between the roughness of the surfaces and their wettability. The next part of this study aims at understanding how the laser-induced surface roughness affects the wetting behavior of the glass surfaces.

3.2. Impact of Texture Period on Wettability

In Figure 7, the measurements of contact angle are presented as a function of periodicity and number of passages in different curing environments.

Before texturing, the reference surfaces exposed to nitrogen, air, and hot water showed a hydrophilic behavior, with contact angles significantly lower than 90°. The hydrophilicity was more pronounced on surfaces exposed to nitrogen, with a contact angle of around 53°, and less pronounced on those exposed to water, with an angle of around 63°. In contrast, the chemically treated surface had a contact angle of 95°, indicating a hydrophobic behavior.

After texturing, we observed a more significant decrease in contact angles of hydrophilic surfaces compared to reference surfaces, with an increase in periodicity and number of passages, resulting in a significant increase in

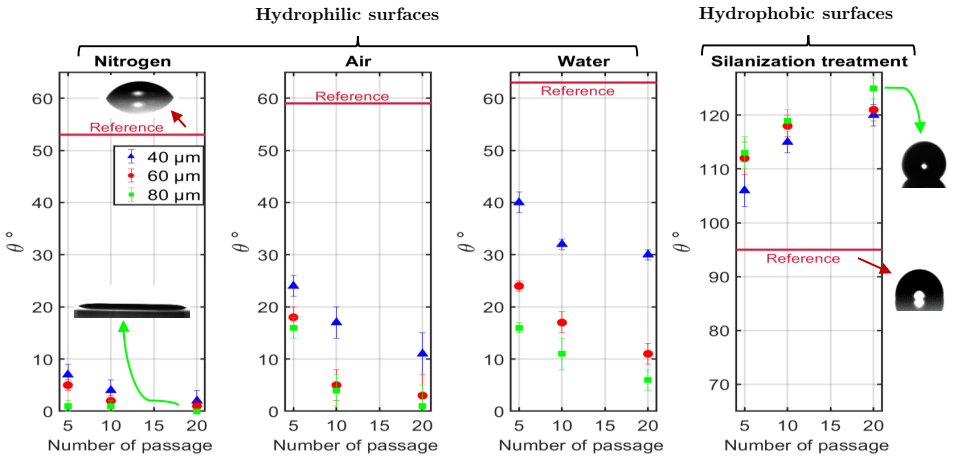

Figure 7: Contact angle measurements on flat glass surfaces irradiated with a fluence of 13.6 J/cm^2 for periodicities of 40 μm (triangles), 60 μm (circles), and 80 μm (squares) in nitrogen, air, and water curing environments, and after silanization treatment (from left to right). The red lines represent the contact angles on the surfaces before irradiation.

the hydrophilicity of these surfaces. On the other hand, for hydrophobic surfaces, an increase in periodicity and number of passages led to an increase in contact angles, indicating an increase in hydrophobicity. These results support the hypothesis that surface roughness amplifies the initial wettability of reference surfaces, as reported in previous studies (18; 35).

3.3. The effect of roughness on wettability

After texturing, we found that the roughness of the grooves changes, depending on the laser parameters used. This roughness, in turn, influences wettability.

To demonstrate the impact of surface roughness on wettability, we measured the contact angles of laser-irradiated surfaces at different fluences, numbers of passages, and with a periodicity of 60 μm on air-cured and chemically-treated slides.

As previously shown, at higher fluences and numbers of passages, the grooves become wider and deeper, resulting in decreased contact angle values on hydrophilic reference surfaces after texturing. This indicates that water penetrates into the entire surface created by the large openings.

On silanized surfaces, the contact angle on a non-textured surface was measured at 95°, while for textured surfaces, the angle was greater than 110° and changed with fluence and number of passages. Measurements made 287 days after texturing at 40 μm periodicity with 5, 10 and 20 passages, have shown $[110^o - 125^o]$ contact angle. It confirmed measurements made after 7 days with deviations less that $\pm 5^o$.

4. Wetting Regimes

To study the wetting regimes on the textured surfaces, we calculated the geometrical parameters of roughness and fraction of the wetted surfaces, as well as the hysteresis of the contact angle. We conducted the study for air-cured textured surfaces and chemically treated textured surfaces.

The Wenzel roughness r and Cassie-Baxter fraction f of the textured surfaces were calculated from the morphological profiles, as explained in the diagrams in Figure 2. These parameters were also calculated using the previously measured contact angles and Equations 2 and 3.

Figures 8.a and 8.b show a comparison of the roughness parameters calculated from the observed geometry and contact angle measurements, for two different surface chemistries.

Figure 8.a presents a comparison of the Wenzel roughness r calculated from the contact angles and the Wenzel roughness r calculated from the mor-

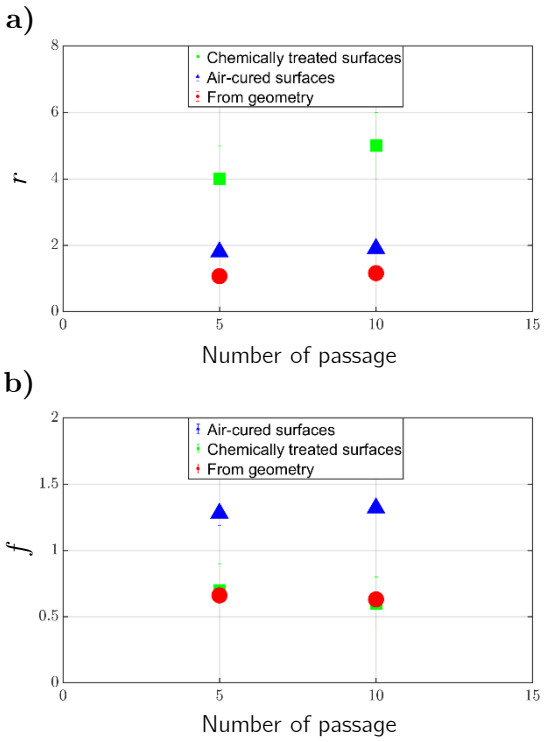

Figure 8: a) Comparison of Wenzel roughness r measured from morphological profiles and calculated from the contact angles of air-cured and chemically treated surfaces using equation(2). b) Comparison of the fraction f of the wetted surface from Cassie-Baxter equation (3) measured from morphological profiles and calculated from the contact angles of air-cured and chemically treated surfaces.

phological profiles of the air-cured and chemically treated surfaces. It can be observed that the roughness calculated from the contact angles deviates from the roughness calculated from the morphological profile for chemically treated surfaces, suggesting that the liquid does not fully fill the grooves, which implies that the Wenzel regime does not match the actual liquid-surface structure. On the other hand, for air-cured surfaces, the roughness calculated from the contact angles is much closer to the roughness calculated from the morphological profile, suggesting that the drops fill the grooves, corresponding to a regime close to the Wenzel regime.

Figure 8.*b* presents the comparison of the Cassie-Baxter fraction f calculated from the morphological profiles and from the contact angles on air-cured and chemically treated surfaces. On the air-cured surfaces, the calculated fraction of wetted surfaces is greater than 1, which is inconsistent and fails to explain the wetting using the Cassie-Baxter regime. However, on chemically treated surfaces, the fraction of wetted surfaces calculated from both the morphological profiles and contact angles are consistent with each other, suggesting that the Cassie-Baxter model is more effective in explaining the wetting observations. These observations are further supported by hysteresis measurements, which were found to be around 13°.

5. Conclusions

In conclusion, our study has demonstrated the versatility of modifying the wettability of flat soda-lime silica glass surfaces through the combination of femtosecond laser irradiation and chemical treatment with a silanization solution. Our results have shown the ability to transform the surface from

hydrophilic to superhydrophilic and ultimately to hydrophobic, with contact angles ranging from below 20° to approaching 125°, emphasizing the crucial role of surface morphology and chemical composition in determining the wettability of a surface and its classification into either a Wenzel or Cassie-Baxter regime.

The present work expands the understanding of glass surface wettability with surface texturing. It offers a solid framework to tune the wettability regime of soda-lime silica glass surfaces with femto-second laser texturing parameters and chemical composition of curing environments.

This work presents exciting possibilities for various applications, including microfluidics, optics, and surface science. With further investigation into the durability and wettability stability of the treated surfaces, we can expect to see an increased use of this technology for solving real-world problems. To explore further the effect of surface texturing and chemical treatment of soda-lime silica flat surfaces, it would be of great interest to focus on curved surfaces. In particular, the control of the internal wettability of millimeter-sized glass tube would be useful for self-cleaning and solid particles removal in the case of an increased hydrophobicity, whereas an increased hydrophilicity would ease fast two-phase flows in milli- or mirofluidic processes.

The aging and long-time evolution of the wetting properties is shown to be controlled with complex chemical processes on textured mettallic surfaces. On glass surfaces the long-time reactivity of functional groups could change the wetting properties. Despite the comforting contact angle measurements done with textured and silanized surface after 287 days, further study would be required to solidify the present conclusions.

References

[1] X. M. Li, D. Reinhoult, M. Crego-Calama, *What do we need for a superhydrophobic surface? A review on the recent progress in the preparation of superhydrophobic surfaces.*, Chem. Soc. Rev., **36**, 1350, (2007).

[2] S. Rasouli, N. Rezaei, H. Hamedi, S. Zendehboudi, and X. Duan *Superhydrophobic and superoleophilic membranes for oil-water separation application: A comprehensive review*, Materials and Design, **204**, 109599, (2021).

[3] Q. Zeng, H. Zhou, J. Huang, and Z. Guo, *Review on the recent development of durable superhydrophobic materials for practical applications*, Nanoscale, **13**, 11734 (2021).

[4] J. Jeevahan, M. Chandrasekaran, G. Britto Joseph, R. B. Durairaj, and G. Mageshwaran, *Superhydrophobic surfaces: a review on fundamentals, applications, and challenges*, J. Coat. Technol. Res. **15**, 231 (2018).

[5] C. Ishino, K. Okumura and D. Quéré, *Wetting transitions on rough surfaces*, J. Europhys. Lett. **68**, 419 (2004).

[6] R. N. Wenzel, *Resistance of solid surfaces to wetting by water*, Ind. Eng. Chem., **38**, 988 (1936).

[7] G. D. Nadkarnf, and S. Garoff, *Reproducibility of contact line motion on surfaces exhibiting contact angle hysteresis*, Langmuir, **10**, 4367, (1994).

[8] A. B. D. Cassie, and S. Baxter, *Wettability of porous surfaces*, Trans. Faraday Soc., **40**, 546 (1944).

[9] H. B. Eral, D. J. C. M. 't Mannetje, and J. M. Oh, *Contact angle hysteresis: a review of fundamentals and applications*, Colloid. Polym. Sci. **291**, 247 (2013).

[10] G. McHale, N. J. Shirtcliffe, and M. I. Newton, *Contact angle hysteresis and super-hydrophobic surfaces*, Langmuir, **20**, 10146 (2004).

[11] M. Liu, S. Wang, and L. Jiang, *Nature-inspired superwettability systems*, Nature Reviews Materials, **2**, 17036 (2017).

[12] P., Bizi-Bandoki, S. Benayoun, S. Valette, B. Beaugiraud, E. Audouard, *Modifications of roughness and wettability properties of metals induced by femtosecond laser treatment*, App. Surf. Sci. **257**, 5213 (2011).

[13] V. Belaud, S. Valette, G. Stremsdoerfer, M. Bigerelle, S. Benayoun, *Wettability versus roughness: Multi-scales approach*, Tribology International, **82**, 343, (2015).

[14] Q. Legrand, S. Benayoun, S. Valette, *Biomimetic Approach for the Elaboration of Highly Hydrophobic Surfaces: Study of the Links between Morphology and Wettability*, Biomimetics, **6**, 38, (2021).

[15] S. Divin-Mariotti, P. Amieux, A. Pascale-Hamri, V. Auger, G. Kermouche, F. Valiorgue, S. Valette, *Effects of micro-knurling and femtosecond laser micro texturing on aluminum long-term surface wettability*, App. Surf. Sci., **479**, 344, (2019).

[16] M. Huff, *Recent Advances in Reactive Ion Etching and Applications of High-Aspect Ratio Microfabrication*, Micromachines **12**, 991 (2021).

[17] M. Pedersen, and M. Huff, *Plasma Etching of Deep, High-Aspect Ratio Features into Fused Silica* J. Microelectromech. Syst. **26**, 448 (2017).

[18] A.-M. Kietzig, S. G. Hatzikiriakos, and P. Englezos, *Patterned Superhydrophobic Metallic Surfaces*, Langmuir **25**, 4821 (2009).

[19] C. Florian, E. Skoulas, D. Puerto, A. Mimidis, E. Stratakis, J. Solis, and J. Siegel, *Controlling the Wettability of Steel Surfaces Processed with Femtosecond Laser Pulses*, ACS Appl. Mater. Interfaces, **10**, 36564 (2018).

[20] B. Wu, M. Zhou, J. Li, X. Ye, G. Li, and L. Cai, *Superhydrophobic surfaces fabricated by microstructuring of stainless steel using a femtosecond laser*, App. Surf. Sci. **256**, 61 (2009).

[21] C.-J. Yang, X.-S. Mei, Y.-L. Tian, D.-W. Zhang, Y. Li, and X.P. Liu, *Modification of wettability property of titanium by laser texturing*, Int. J. Adv. Manuf. Technol., **87**, 1663 (2016).

[22] S. Rung, S. Schwarz, B. Götzendorfer, C. Esen, and R. Hellmann, *Time Dependence of Wetting Behavior Upon Applying Hierarchic Nano-Micro Periodic Surface Structures on Brass Using Ultra Short Laser Pulses* Appl. Sci., **8**, 700 (2018).

[23] A. O. Ijaola, E. A. Bamidele, C. J. Akisin, I. T. Bello, A. T. Oyatobo, A. Abdulkareem, P. K. Farayibi, and A. Asmatulu, *Wettability Transi-*

tion for Laser Textured Surfaces: A Comprehensive Review, Surf. and Interfaces, **21**, 100802 (2020).

[24] M. K. Bernett, and W. A. Zisman, *Effect of Adsorbed Water on Wetting Properties of Borosilicate Glass, Quartz, and Sapphire*, J. Colloid Interface Sci., **29**, 413 (1969).

[25] A. Kanta, R. Sedev, and J. Ralston, *Thermally- and Photoinduced Changes in the Water Wettability of Low-Surface-Area Silica and Titania*, Langmuir, **21**, 2400 (2005).

[26] Y. C. Araujo, P. G. Toledo, V. Leon, and H. Y. Gonzalez, *Wettability of Silane-Treated Glass Slides as Determined from X-Ray Photoelectron Spectroscopy*, J. Colloid Interface Sci., **176**, 485 (1995).

[27] S. Takeda, K. Yamamoto, Y. Hayasaka, and K. Matsumoto, *Surface OH group governing wettability of commercial glasses*, J. of Non-Crystalline Solids, **249**, 41 (1999).

[28] M. Martínez-Calderon, A. Rodríguez, A. Dias-Ponte, M. C. Morant-Miñana, M. Gómez-Aranzadi, and S. M. Olaizola, *Femtosecond laser fabrication of highly hydrophobic stainless steel surface with hierarchical structures fabricated by combining ordered microstructures and LIPSS*, J. Applied Surface Sci., **374**, 81 (2016).

[29] X. Sedao, M. Lenci, A. Rudenko, N. Faure, A. Pascale-Hamri, J.P. Colombier and C. Mauclair, *Influence of pulse repetition rate on morphology and material removal rate of ultrafast laser ablated metallic surfaces*, J. Optics and Lasers in Engineering, **116**, 68 (2019).

[30] V. Laurent, *Mouillabilité des surfaces superhydrophobes et superoléophobes*, J. Techniques de l'ingénieur, base documentaire : TIP553WEB, (2017).

[31] H. B. Eral and D. J.C.M. 'T Mannetje and J. M. Oh, *Contact angle hysteresis: A review of fundamentals and applications*, J. Colloid and Polymer Sci., **291**, 247 (2013).

[32] R. Di Mundo and F. Palumbo, *Comments regarding 'an essay on contact angle measurements*, J. Plasma Processes and Polymers, **8**, 14 (2011).

[33] H. Kamusewitz and W. Possartt, *The static contact angle hysteresis obtained by different experiments for the system PTFE/water*, J. International journal of adhesion and adhesives, **5**, 211 (1985).

[34] V. Hisler, H. Jendoubi, C. Hairaye, L. Vonna, V. Le Houérou, F. Mermet, M. Nardin, and H. Haidara, *Tensiometric Characterization of Superhydrophobic Surfaces As Compared to the Sessile and Bouncing Drop Methods*, J. Langmuir, **32**, 7765 (2016).

[35] Y. Liu and C. H. Choi, *Condensation-induced wetting state and contact angle hysteresis on superhydrophobic lotus leaves*, J. Colloid and Polymer Science, **291**, 437 (2013).